Increased Fracture Toughness in a 300 Grade Maraging Steel as a Result of Thermal Cycling

STEPHEN D. ANTOLOVICH, ASHOK SAXENA, AND G. R. CHANANI

Systematic changes in the fracture toughness of a 300 grade commercial maraging steel were obtained using a non-standard heat-treating process. Microstructures consisting of variable amounts of retained austenite in an aged martensitic matrix were produced. A mathematical model is presented relating these toughness values to the properties of the individual constituents. Increases in fracture toughness resulting from the non-standard heat-treatment were attributed to the nature of the distribution of the tough phase (retained austenite) in a brittle matrix of precipitation hardened martensite. In some cases, a strain-induced transformation to martensite was observed which greatly added to the toughness. Some improvements in fatigue crack propagation characteristics also resulted from this heat treatment.

THE operating loads in modern structures are decided on the basis of properties such as strength, toughness and fatigue crack propagation (FCP) behavior. Recently, there has been some success in improving fracture toughness with negligible reductions in strength. Some examples are: 1) A very effective crack arrest is observed due to decohesion that occurs ahead of the tip of a crack approaching the brittle-ductile interface in a metal composite.[1-3] 2) Energy absorption due to the austenite (A) to martensite (M) transformation which occurs concurrently with plastic straining, results in a much higher toughness for TRIP steels.[4,5] 3) Large improvements in fracture toughness have also been obtained by effective crack arrest mechanisms in micro-duplex structures.[6-10]

Despite over a decade of commercial availability of maraging steels, there has been limited success in improving their fracture toughness. The higher strength maraging alloys, namely the 300 and 350 grades, fail catastrophically in the presence of flaws. This paper reports the effects of introducing a finely distributed tough phase (retained austenite) in an aged martensitic matrix of 300 grade maraging steel on the plane-strain fracture toughness (K_{IC}) and on other mechanical properties.

I. PREVIOUS STUDIES

Decker, Eash, and Goldman[11] were the first to observe the very effective precipitation hardening that occurs in iron-nickel martensites on aging at intermediate temperatures when elements such as molybdenum, titanium, and cobalt are added to the alloys. Cobalt in the presence of other elements provides a faster hardening response[12-14] but in itself produces little hardening.*

*For a detailed background on physical metallurgy of maraging steels, the reader is referred to an excellent review by Floreen.[15]

STEPHEN D. ANTOLOVICH and ASHOK SAXENA are Associate Professor and Graduate Research Assistant, respectively, Department of Materials Science and Metallurgical Engineering, University of Cincinnati, Cincinnati, Ohio. 45221. G. R. CHANANI, formerly Postdoctoral Fellow, Department of Materials Science and Metallurgical Engineering, University of Cincinnati is Senior Research Engineer, Northrop Aviation Corp., Hawthorne, Calif. 90250.

Manuscript submitted July 27, 1973.

Goldberg has studied the phase transformations in 300 grade maraging steel occurring during repeated heating and cooling.[16-18] Relying heavily on dilatometric and microscopic observations, he has proposed that on heating the sluggishness of M → A transformation permits M to persist well into the two phase (ferrite + austenite) equilibrium region. Along with the simultaneous growth of austenite and ferrite (F), austenite that is rich in alloying elements also nucleates on precipitates that had formed during heating. At the austenite finish temperature (A_f), the alloy is completely austenitic but very heterogeneous in composition. If the alloy is immediately cooled so that homogenization is minimized, the alloy-rich austenite remains untransformed, while the alloy-depleted austenite transforms to martensite. During the heating part of the cycle, diffusion occurs which tends to homogenize the chemical composition of the austenite. Thus, the volume of retained austenite after each thermal cycle between room temperature and a temperature above A_f is very sensitive to the heating rate. It was observed[16] that at very high heating rates (on the order of 60°C/s and higher) the M → A transformation is diffusionless and, thus, only minor changes in composition occur. Under such conditions retained austenite does not form. At very slow heating rates homogenization of the austenite can be expected to occur as a result of extensive diffusion, and again very little retained austenite forms. At appropriate intermediate heating rates some additional retained austenite forms after each successive thermal cycle.

II. EXPERIMENTAL PROCEDURE

A 7.6 cm diam billet of 300 grade maraging steel was obtained from Universal Cyclops in the solution annealed and centerless ground condition. The chemical composition is given in Table I. The billet was homogenized at 1150°C for 6 h in a slightly oxidizing atmosphere and hot rolled to a 3.8 cm flat plate. Dilatometric specimens 25 mm long × 6.4 mm diam were machined keeping the direction of rolling parallel to the specimen axis. Compact Tension (CT) specimens 13 mm thick and Single-Edge-Notch (SEN) specimens 4.8 mm thick were machined such that the rolling direction was parallel to the loading direction. Tensile coupons were machined from the broken halves of the

CT specimens such that they were parallel to both the crack plane and the direction of crack propagation.

The equipment used for dilatometric studies was similar to that used by Goldberg.[16] The heating rate used in this study was 0.33°C/s and was controlled using a programmable temperature controller. Fracture toughness tests, using CT specimens, were performed following the ASTM specifications[19] using a 220 kN MTS Universal testing system in the load control mode. The FCP studies were carried out using the SEN specimens. Tensile testing was done using a 90 kN Instron machine. Strain was measured using strain gages directly bonded to the samples.

Metallography was performed by mechanically polishing and subsequently etching using a 5 pct nital solution. Two stage replicas were prepared from both polished and fractured surfaces for electron microscopy.

III. RESULTS AND DISCUSSION

A. Dilatometry and Microstructure

Fig. 1 shows a typical dilatometric heating and cooling curve obtained from an annealed specimen heated to 825°C in air at 0.33°C/s, held for two hours, and subsequently cooled to room temperature. The slight dip between P_S (precipitation start temperature) and A_S (austenite start temperature) has been attributed to the formation of precipitates that normally form during aging.[16] The large contraction between the A_S and A_f (austenite finish) is a consequence of transformation to austenite. The two hour hold at 825°C homogenized the austenite. The A_S, A_f, M_S, and M_f (martensite finish temperature) for this alloy were found to be 615, 781, 156, and 60°C, respectively. Note that the M_f is above room temperature, thus implying the structure in the as-received condition is martensitic.

The large degree of microsegregation that develops during heating is revealed by the dilatometric cooling curves taken from specimens that were subjected to repeated thermal cycling between room temperature and 825°C. In the case of thermal cycling, the hold period at 825°C was reduced to two minutes to *minimize* homogenization. Fig. 2 shows the dilatometric curves for the first five thermal cycles. Up to four cycles the A_S decreased and the M_S increased. In the fifth cycle there was a slight decrease in the M_S and a corresponding increase in the A_S (Fig. 3). A plausible explanation is that, after four cycles, the matrix is so depleted in alloying elements that it can no longer undergo significant precipitation during heating while the composition of the more depleted regions in the austenite become more homogeneous leading to a decrease in M_S.

The important observation here is that right from the first cycle the M_f drops below room temperature suggesting an incomplete A→M transformation. Goldberg[16] has suggested that retained austenite, once formed, remains untransformed during subsequent cycling.

Fig. 4 shows replica electron micrographs from samples that were given various thermal treatments. Fig. 4(*a*) was taken from a sample that was conventionally heat-treated and no unusual features are present. After the first cycle, (Fig. 4(*b*)), a lamellar phase

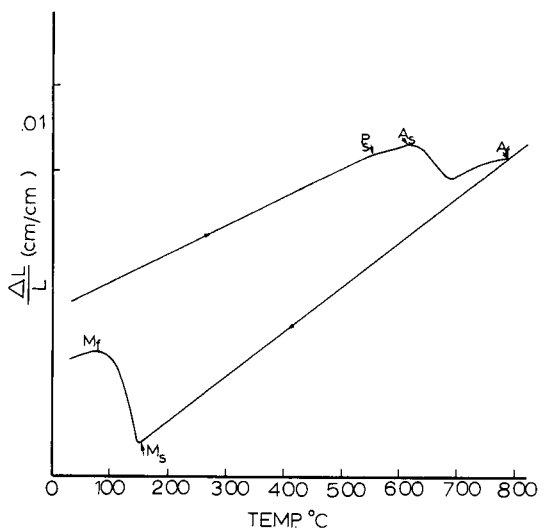

Fig. 1—Dilatometric heating and cooling curve of as-received 300 grade maraging steel, heated to 825°C at 0.33°C/s, held for 2 h and furnace cooled.

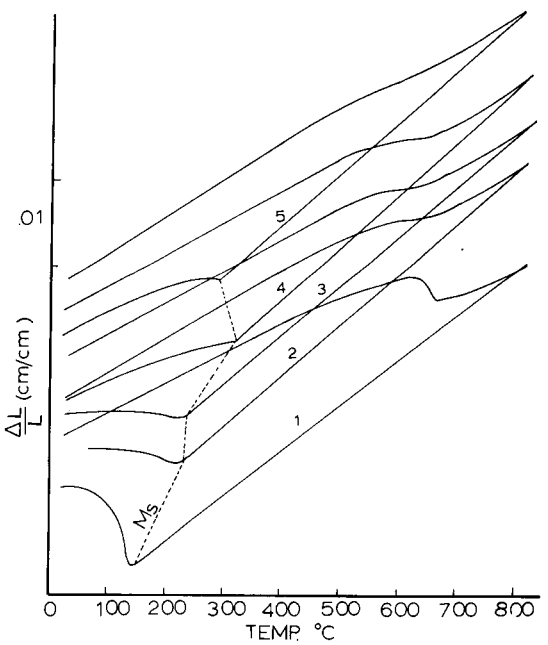

Fig. 2—Sequential dilatometric heating and cooling curve for a specimen heated to 825°C at 0.33°C/s, held for 2 min and furnace cooled. The numbers represent the number of cycles after completion.

Table I. Chemical Composition of 300 Grade Maraging Steel (Wt Pct)

Al	Ti	C	Mn	Si	S	P	B	Zr	Ca	Ni	Mo	Co	Fe
0.11	0.69	0.006	0.05	0.07	0.003	0.002	0.0027	0.016	0.0003	18.8	4.94	9.07	bal

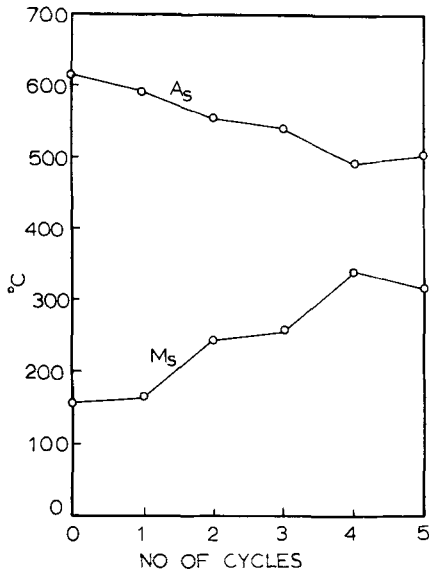

Fig. 3—Change in the M_S and A_S as a function of the number of thermal cycles.

appears in the matrix. This has been identified as retained austenite.[16] Additional retained austenite forms as a result of repeated thermal cycling as can be seen from micrographs 4(*c*), (*d*), and (*e*).

The dilatometric curves of Fig. 2 show that after the second cycle, the A_f exceeded 835°C implying that some martensite remained untransformed at that temperature. This in turn suggests the presence of some highly solute depleted martensite regions (probably located adjacent to the freshly formed retained austenite) which, as a result of exposure to high temperature tend to spheroidize to reduce surface energy. Fig. 4(*e*) illustrates such a microstructure.

The volume percent of retained austenite was determined by standard quantitative metallography using the linear intercept method.[20] It was observed that after one, four, ten and thirty cycles, 17.8, 38, 57.5 and 79.5 vol. pct retained austenite was present.

To roughly assess the stability of the retained austenite, thermally cycled specimens were quenched in liquid nitrogen and subsequently aged for $3\frac{1}{2}$ h at 490°C. No change in the structure of retained austenite was observed leading to the conclusion that M_f for cycled maraging steel lies below −196°C.

B. Mechanical Properties

Table II lists all the mechanical properties studied (excluding FCP properties). All results represent an average of three tests performed on specimens in the same condition. Variations from mean values are also indicated in the table.

1. TENSILE STRENGTH AND HARDNESS

Typical true-stress vs true-strain curves for the various heat treatments employed are shown in Fig. 5. The average tensile properties are listed in Table II. The tensile strength decreased steadily with additional thermal cycling while the percent elongation, reduction in area, and strain hardening exponent increased. The loss in tensile strength from conventionally treated material to material that was cycled once was on the order of 15 pct. This may be attributed to the presence of retained austenite which caused a decrease in flow stress, and consequently a decrease in strength. As an approximation, the tensile strength can be calculated from the well-known rule of mixtures using the following equation:

$$\sigma_{uc} = \sigma_{ut} V_t + \sigma_{ub}(1 - V_t) \quad [1]$$

where

σ_{uc} = tensile strength of cycled maraging steel.
σ_{ut} = tensile strength of maraging steel in austenitic condition (tough phase). The value of 848 MPa is taken from Ref. 21.
σ_{ub} = tensile strength of aged martensite.
V_t = volume fraction of austenite.

Figure 6 shows there is good agreement between Eq. [1] and experiment.

2. FRACTURE BEHAVIOR

Large increases in fracture toughness were observed as a result of thermal cycling as is evident from Fig. 7 where the fracture toughness is plotted as a function of the number of cycles. K_{IC} increased from 77 MPa$\sqrt{m}$ * in the solution annealed and aged condition to 116 MPa$\sqrt{m}$ for the solution annealed, thermally cycled once, and aged condition (an increase of 52 pct). To illustrate the significance of the results, the square of the ratio of the toughness to the yield strength, which is an index of the maximum crack size that can be tolerated at the yield stress, is plotted against σ_{ys} in Fig. 8 for the family of maraging steels. The superiority of the thermally cycled maraging steel is clearly exhibited by the high toughness-to-strength ratio at those strength levels. A valid K_{IC} could not be measured beyond one cycle using 13 mm thick specimens and hence data is shown only for the solution annealed and aged as well as for the singly cycled and aged conditions. Since the fracture mode changed from abrupt to gradual, other indices of toughness based on maximum load and original crack length (K^o_{max}) and maximum load and instantaneous crack length (K^i_{max}) were used in an attempt to illustrate this behavior. These indices have been used previously for high toughness materials.[2,4,5] The fracture toughness, as measured by either K^o_{max} or K^i_{max}, does not increase much between one and four cycles after which a large somewhat anomalous increase is observed for ten cycles.

The gradual nature of crack extension resulting from cycling is best illustrated by means of crack growth resistance, or *R* curves. The *R* curve concept basically represents an equilibration between applied loads tending to propagate the crack and resistance to propagation as manifested by development of plasticity at the crack tip. This concept is discussed more fully elsewhere[23] and has been used previously by one of the authors (SDA) to illustrate similar behavior.[1] Typical *R* curves are plotted in Fig. 9. The *R* curve for material in the solution annealed and aged condition rises vertically and at a critical point catastrophic fracture occurs. In contrast, the *R* curves for the cycled material continually rise with increasing crack length, illustrating the gradual nature of crack exten-

*MPa$\sqrt{m}$ can be converted to the more familiar engineering unit ksi$\sqrt{in.}$ by dividing by 1.09.

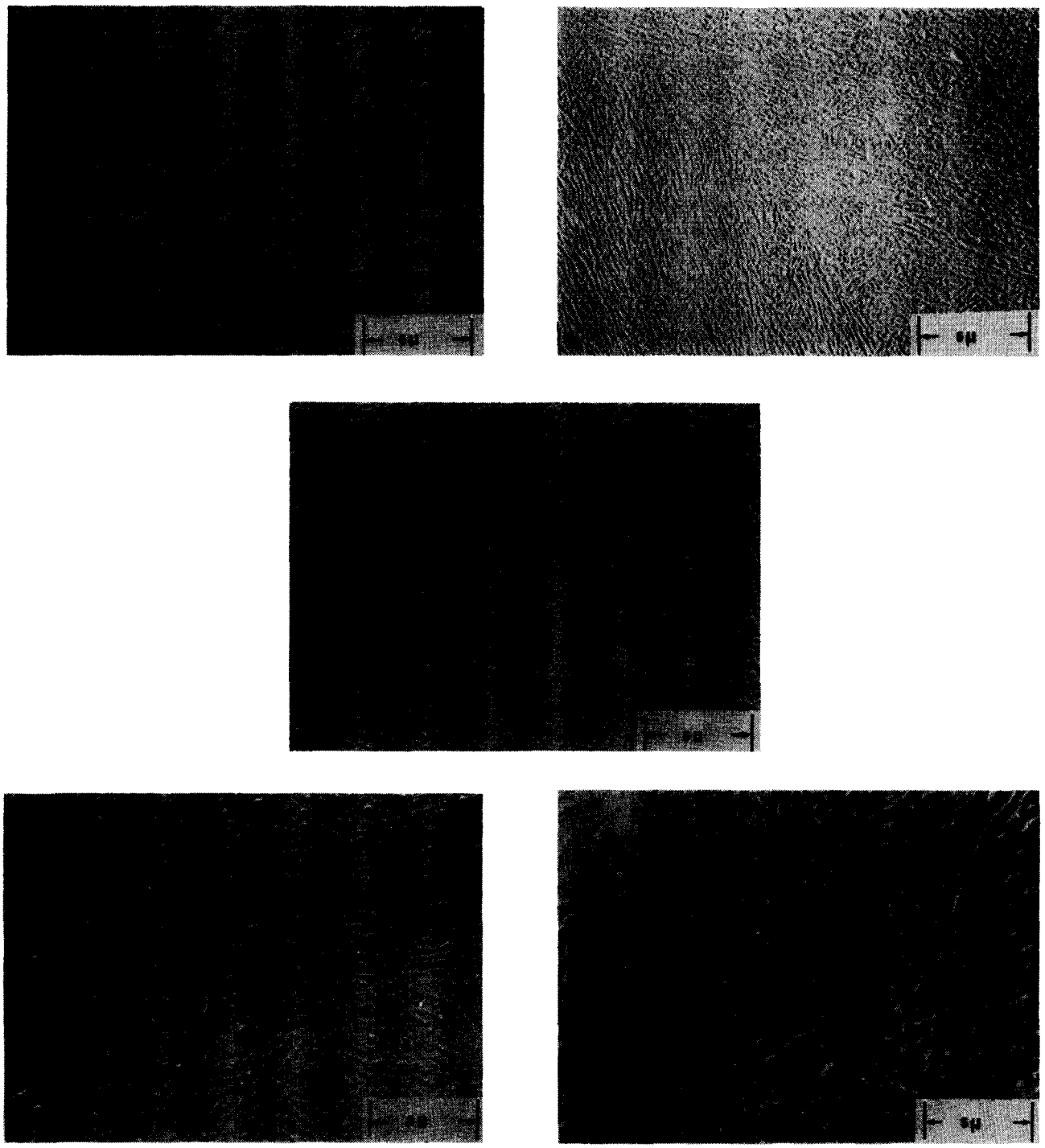

Fig. 4—Electron replica micrographs of 300 grade maraging steel (*a*) solution annealed, (*b*) thermally cycled one, (*c*) four, (*d*) ten and (*e*) 30 times. All samples were aged for 3½ h at 490°C. after the indicated treatments.

sion for this treatment. The effect of only a single cycle on the resistance to fracture is most striking.

Fractographic examinations of the fracture surfaces were made to help understand the mechanism of fracture of maraging steel with different heat treatments. Figure 10 shows some typical fractographs taken from specimens that were conventionally treated [9]Fig. 10(*a*)), cycled once (Fig. 10(*b*)), and cycled ten times (Fig. 10(*c*)). In the solution annealed and aged condition the fracture surface exhibits equiaxed dimples of various sizes which is consistent with results obtained by other investigators.[24] Figure 10(*b*) shows large ductile dimples with evidence of ripples and serpentine glide. Towards the top of the fractograph there is a region very similar in appearance to that of the solution annealed and aged structure. The local direction of crack propagation is from the brittle to the ductile region and it seems probable that the ductile area corresponds to a region dominated by retained austenite and which, by its capacity to plastically deform, relaxes the stresses in the brittle constituent (aged martensite). Such features were frequently encountered in replicas taken from regions that underwent stable fracture. The fracture surface of specimens cycled ten times frequently exhibited large fragmented particles (Fig. 10(*c*) is a typical example) surrounded by a ductile region.

Table II. List of Mechanical Properties

Heat Treatment	Hardness R_c	K_{IC} MPa$\sqrt{m}$	K°_{max} MPa$\sqrt{m}$	K^{i}_{max} MPa$\sqrt{m}$	UTS MPa	True Strain at Necking† ϵ_u	True Strain at Fracture ϵ_f	Pct Reduction in Area
1. Solution annealed and aged.	53.5 ± 1	77^{+2}_{-1}	77^{+2}_{-1}	86^{+4}_{-3}	1944 ± 28	0.017	0.256	22.2
2. Solution annealed cycled once and aged.	47 ± 1	116^{+2}_{-1}	124^{+3}_{-1}	165^{+8}_{-5}	1655^{+28}_{-14}	0.025	0.350	29.3
3. Solution annealed cycled four times and aged	43.5 ± 0.5	*	123^{+4}_{-1}	166 ± 6	1538 ± 41	0.062	0.570	43.5
4. Solution annealed cycled ten times and aged	37 ± 1.5	*	146 ± 7	247 ± 28	1338^{+41}_{-82}	0.190	0.772	55.0

*Not a valid plane-strain fracture toughness measurement. ASTM thickness requirement was not met.

†The true strain at necking (*i.e.*, the total uniform strain) is identical to the strain hardening exponent n for the materials whose stress-strain curves are given by $\sigma = K\epsilon^n$ where K is the strength coefficient.[29]

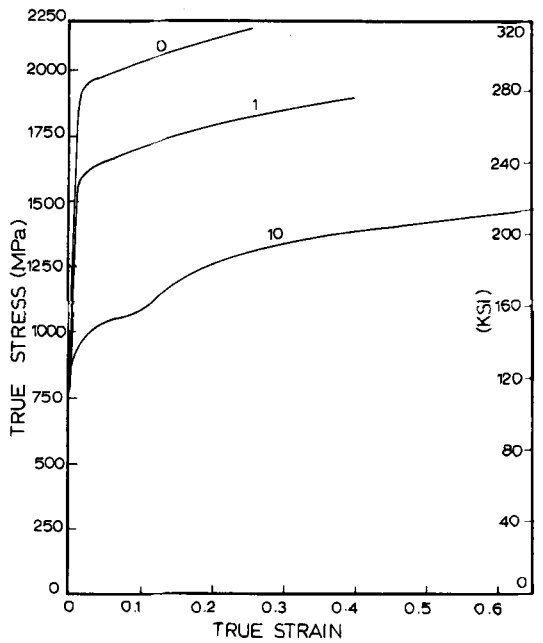

Fig. 5—Typical true stress vs true strain curves. The numbers on the curves indicate the number of cycles.

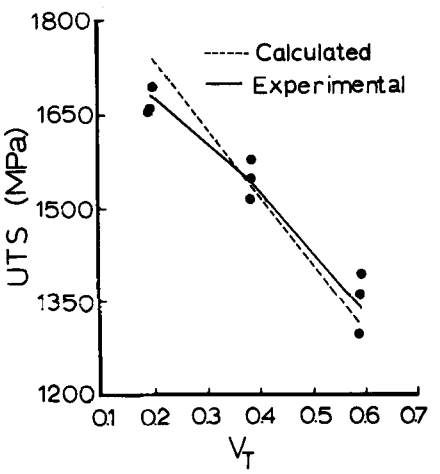

Fig. 6—Tensile strength of cycled and aged steel as a function of the volume fraction of retained austenite.

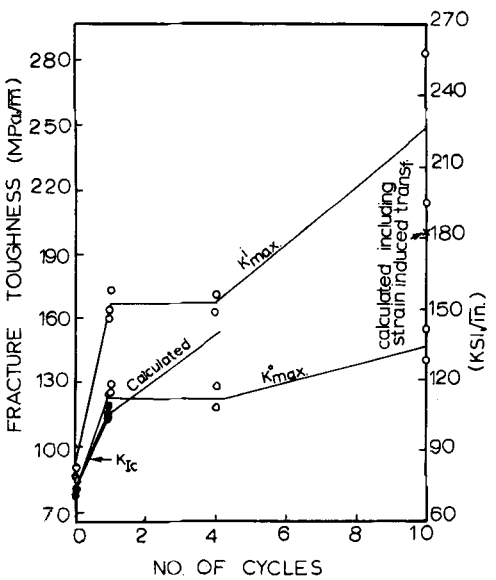

Fig. 7—Variation in fracture toughness as a function of cycles. Valid K_{IC} tests could not be performed beyond one cycle.

These particles are believed to be nitrides and carbides of the alloying elements.[25,26] It is our feeling that due to repeated thermal cycling and aging, precipitates coarsen to form large particles, which subsequently dominate the fracture appearance.

The way in which the presence of retained austenite aids in improving the fracture toughness is not completely clear at this time. The mechanism of failure in aged maraging steels is predominately by void nucleation and growth. The crack extends as these voids begin to impinge and reduce the structural integrity within the plastic enclave. When retained austenite is present, an additional increment of plastic work must be done if the voids in the aged martensite are to link up and the material is effectively toughened. The role of the retained austenite may then be viewed as limiting the nucleation of emissary cracks ahead of the main crack front. This process is illustrated schematically in Fig. 11.

It is of interest to account for this large improvement in fracture toughness in terms of a mathematical model. Unfortunately, little progress at the present time has been made towards quantitative development of micromechanics equations for two phase microstructures. In the past, some workers[8,26] have used Hahn and Rosenfield's[27,28] expression to estimate the fracture toughness:

$$K_{IC} = \sqrt{(\tfrac{2}{3} E \sigma_{ys} n^2)} \qquad [2]$$

where

E = Elastic Modulus.
σ_{ys} = yield strength.
n = strain hardening exponent.

The correlations with experimentally determined values have not always been satisfactory. In the present study, considering the material that was cycled once and using the mechanical property data given in Table II, a value of 368 MPa$\sqrt{m}$ is calculated using Eq. [2]. This represents a gross over-estimate of what was actually observed. The lack of agreement with Eq. [2] is perhaps not surprising since it seems improbable that fracture toughness can be correlated solely to macroscopic mechanical properties of multiphase alloys without specifically considering the mechanical properties and distribution of each phase. A calculation taking the mechanical properties of both constituents into account and based on the energy dissipated by a slowly moving crack is presented below.

Consider a two phase system in which the phases are well distributed: the total energy dissipated per unit area crack extension can be approximated by the algebraic sum of the energies of the individual phases combined in proportion to their volume fraction:

$$G_{IC}^{c} = G_{IC}^{t} V_t + G_{IC}^{b}(1 - V_t) \qquad [3]$$

G_{IC}^{c}, G_{IC}^{t} and G_{IC}^{b} represent the energies dissipated per unit area crack extension by the "composite" (cycled and aged), the tough (retained austenite) and the brittle (aged martensite) materials respectively. Using the well-known relationship between the crack extension force G_{IC} and the critical plane-strain stress intensity parameter K_{IC}

$$G_{IC} = \frac{K_{IC}^2}{E}(1 - \nu^2) \qquad [4]$$

where ν = Poisson's ratio, and substituting into Eq. [3], the following expression is obtained:

$$K_{IC}^{c} = \left[\frac{E}{1 - \nu^2}\{G_{IC}^{t} V_t + G_{IC}^{b}(1 - V_t)\}\right]^{1/2} \qquad [5]$$

G_{IC}^{b} has been experimentally measured, but experimental determination of G_{IC}^{t} would require an inconveniently large sample: hence an estimate of G_{IC}^{t} must be made. The mode of failure of retained austenite, when present in small quantities in a brittle matrix, is probably near plane-strain because of the constraint of the brittle material puts on it. A method for estimating G_{IC}^{t} is outlined below.

Goodier and Field[30] have derived an expression for calculating the plastic energy dissipated by a propagating crack in a plate of unit thickness which, for limited plasticity, should be approximately the same as the crack extension force:

$$G = \frac{dW_p}{da} = \frac{2}{\pi}(\kappa + 1)(1 + \nu) Ea\left(\frac{\sigma_{ys}}{E}\right)^2 f(t) \qquad [6]$$

where

$\kappa = 3 - 4\nu$ for plane-strain.

$t = \dfrac{\sigma}{\sigma_{ys}}$ (σ is the remote stress).

$$f(t) = \frac{\pi t}{2}\tan\frac{\pi t}{2} - \ln\sec\frac{\pi t}{2}$$

This model assumes that the material is non-strain hardening and that the yield zone is of the type described by Dugdale[31] based on Muskhelishvilli's[32] solution to the center crack problem. For further calculations, a value must be chosen for the half-crack length a. This can be done without any loss of generality if the remote stress is chosen correspondingly.

a) Calculation of G_{IC}^{b}. The critical remote stress, σ, is given by:

$$\sigma = \frac{K_c}{\sqrt{\pi a}} \qquad [7]$$

Substituting $K_c = K_{IC}^{b}$ and $a = 1.27$ cm a critical stress of 384.1 MPa is computed. Substituting $\nu = 0.28$, $\kappa = 1.88$,

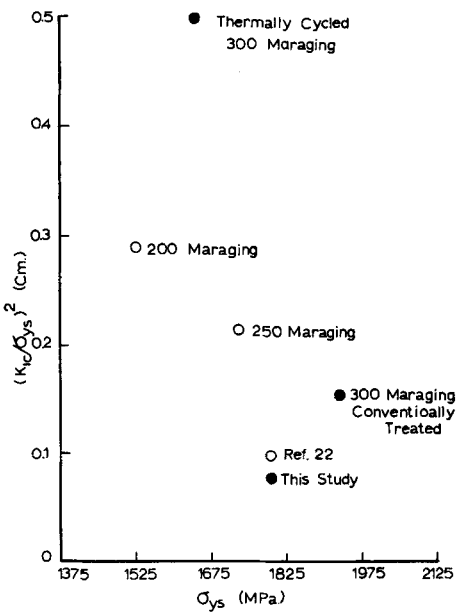

Fig. 8—Yield strength normalized toughness vs yield strength for maraging steels.

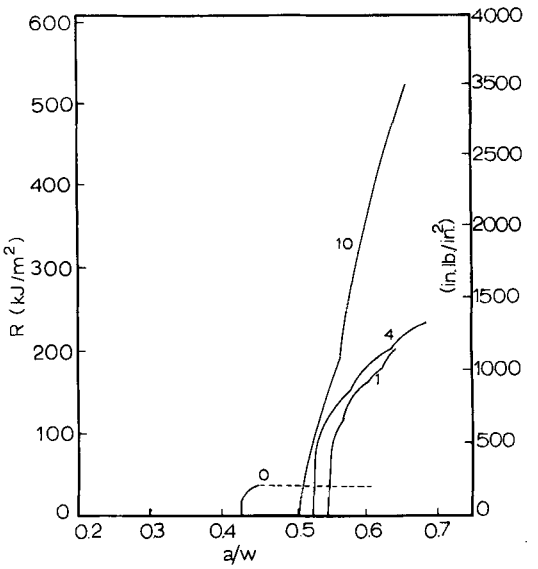

Fig. 9—Crack growth resistance curves as a function of crack length. The numbers represent the number of thermal cycles.

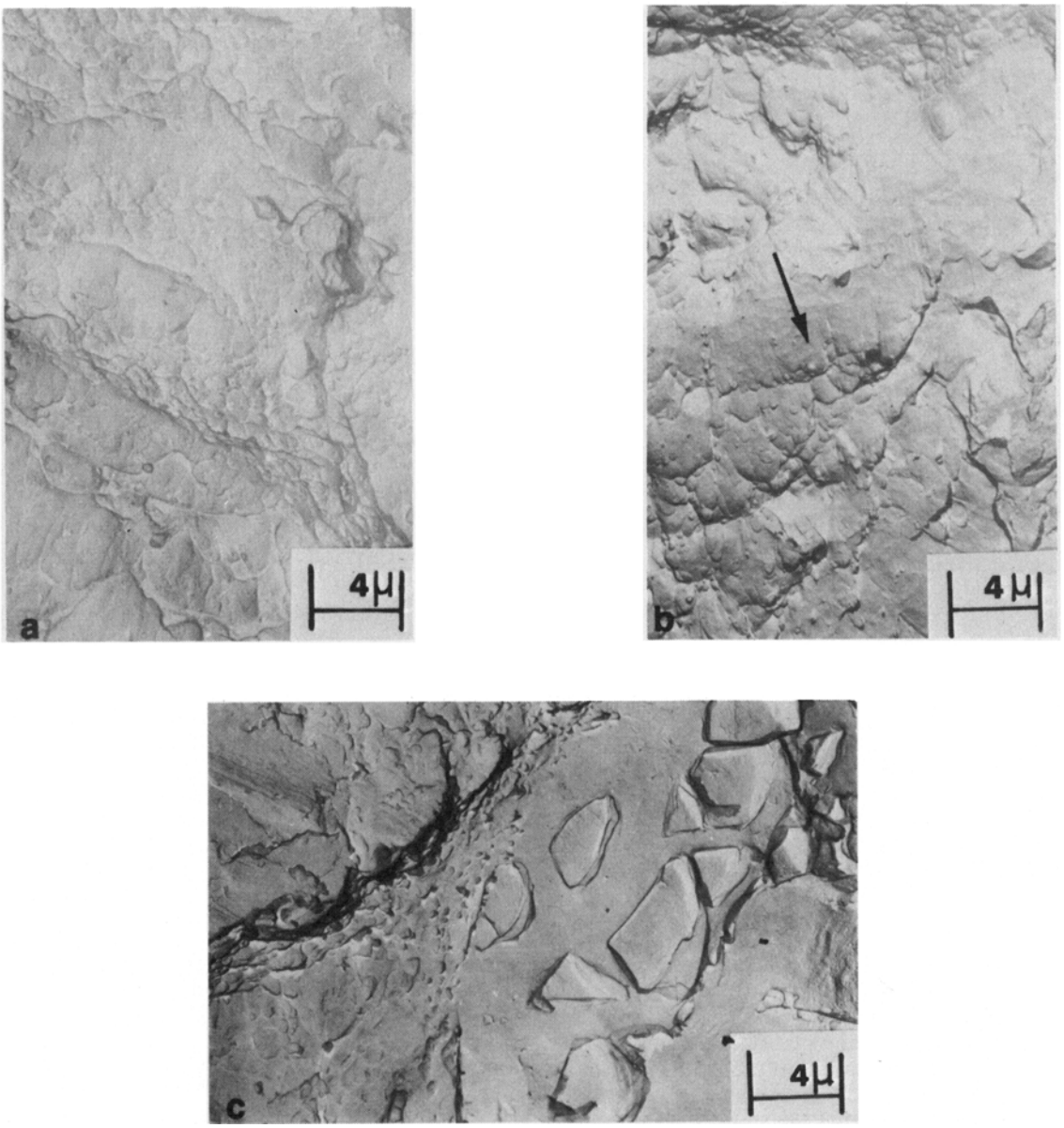

Fig. 10–Typical fractographs from specimens that were (*a*) solution annealed and aged, (*b*) cycled once and aged and (*c*) cycled ten times and aged.

$E = 19.3 \times 10^{10}$ Pa, $\sigma_{ys} = 1931$ MPa, and using Eq. [6] we have $G_{IC}^{b} = 29.4$ kJ/m^2. The measured value of G_{IC}^{b}, obtained from converting K_{IC}^{b} measured experimentally, (by using Eq. [4]), is 28.4 kJ/m^2 which compares well with the calculated value.

b) Calculation of G_{IC}^{t}. The critical remote stress in a semi-infinite sheet of singly cycled and aged maraging steel is calculated to be 583 MPa using Eq. [7]. Because the elastic properties are substantially the same for both constituents, the remote stress at which the tough phase cracks under the constraint from the brittle phase is also assumed to be 583 MPa. Substituting $\sigma_{ys} = 710$ MPa (Ref. 21) and the elastic constants used previously, Eq. [6] yields the result:

$$G_{IC}^{t} = 252 \text{ kJ/m}^2$$

Substituting values for G_{IC}^{b}, G_{IC}^{t} and V_t into Eq. [5] yields a value of 119 MPa$\sqrt{\text{m}}$ for the material that was cycled once and aged. This is in excellent agreement with the experimental value of 116 MPa$\sqrt{\text{m}}$. While the specimen fabricated from the material that was cycled 4 times was not under plane-strain constraint it is of interest to calculate the toughness using Eq. [5]. The result is 154 MPa$\sqrt{\text{m}}$ which appears reasonable and lends further credence to the calculation. The material that was cycled 10 times exhibited a strain-induced transformation and a different model of the fracture process must be invoked.*

*With each successive cycle, the retained austenite that formed previously becomes depleted in alloying elements by diffusion and eventually a point is reached where it can transform to martensite upon the application of stress. In addition, after a number of cycles the retained austenite that does precipitate does so from a generally alloy-depleted matrix and it too may transform upon application of stress. Thus only a portion of the retained austenite is expected to transform on stressing and this behavior was in fact observed.

c) Strain Induced Austenite → Martensite Transformation. To determined whether the retained austenite transformed to martensite during deformation, frac-

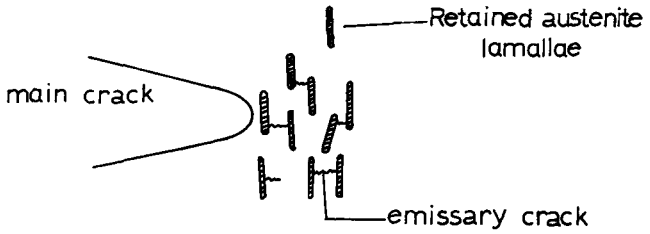

Fig. 11—Tentative mechanism depicting retained austenite blocking small emissary cracks in the plastic zone ahead of the main crack front.

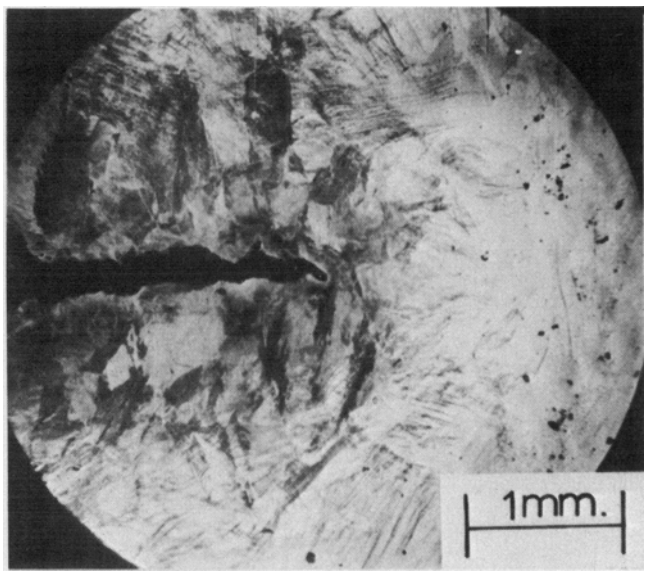

Fig. 12—Martensite formation around crack tip of partially fractured specimen that had been cycled 10 times prior to aging.

tured tensile specimens from each of the heat treatments were aged at 490°C for $3\frac{1}{2}$ h. Microhardness readings were taken from the heavily deformed region and the region not subjected to any plastic deformation. The hardness results are listed in Table III. No change in hardness was observed for samples cycled one and four times, but samples cycled ten times aged to maximum hardness in the deformed region, strongly suggesting the occurrence of a strain-induced transformation from austenite to martensite, similar to that which occurs in TRIP alloys.[4,5]

A partially fractured compact tension specimen of material that had been cycled ten times was aged, mounted, and polished after sectioning at the midthickness. Preferential etching of what is assumed to be transformed martensite around the crack tip delineated the plastic zone boundary as shown in Fig. 12.

It would be of interest to estimate the increase in fracture toughness due to the strain-induced transformation. Antolovich and Singh[4] have derived such an expression for the reduction in strain energy associated with martensite formation ahead of a crack:

$$\Delta U^{A\rightarrow M} = \left(\sigma_M \frac{\epsilon_{IS}}{\sqrt{3}}\right)\left(\pi\beta h^2 B\right)\cdot \bar{V}_M \qquad [8]$$

where

$\Delta U^{A\rightarrow M}$ = strain energy associated with the A → M transformation within the plastic zone.

ϵ_{IS} = invariant shear strain associated with the transformation.

σ_M = tensile stress at which the martensite forms.

2h, 2βh = height and width of the martensite zone (Fig. 12).

B = specimen thickness.

$\bar{V}_M$ = volume fraction of strain induced martensite in the martensite zone.

Using Eq. [8], an expression for the incremental fracture toughness has been derived:[4]

$$\Delta G^{A\rightarrow M} = \frac{\epsilon_{IS}\pi \bar{V}_M \beta \alpha^2 P^4}{\sqrt{3}\,\sigma_M^3 B^4 W^4}\; aF\left(\frac{a}{W}\right) \qquad [9]$$

where

α = half-height of martensite zone divided by the square of the ratio of the stress intensity parameter to the yield stress.

P = load on the specimen.

$$F\left(\frac{a}{W}\right) = 2Y^4\left(\frac{a}{W}\right) + 4Y^3\left(\frac{a}{W}\right)a\,\frac{\partial Y(a/W)}{\partial a}$$

$Y\left(\frac{a}{W}\right)$ = dimensionless calibration function.

W = specimen width.

The following typical values were determined from a specimen that was cycled ten times:

σ_M = 1103 MPa*

$\frac{a}{W}$ = 0.625

$F\left(\frac{a}{W}\right) = 11.52\times 10^5$

ϵ_{IS} = 0.20 (Ref. 33)

P = 26,688 N

α = 0.034 (from metallography)

β = 0.36 (from metallography)

$\bar{V}_M$ = 0.27 (quantitative metallography)

*σ_M is the stress at which the dip in the stress strain diagram for the material cycled ten times occurs which probably is caused by the onset of strain induced $A \rightarrow M$ transformation.

On substituting the above values into Eq. [9] the toughness increment associated with the strain-induced transformation is calculated to be:

$$\Delta G^{A\rightarrow M} = 39.4\ \text{kJ/m}^2$$

Adding the toughness contributions from the two phases and from the strain induced transformation, the fracture toughness of maraging steel cycled ten times prior to aging is calculated to be 201 MPa$\sqrt{\text{m}}$. A curve showing the predicted values of K_{IC}^c is drawn in Fig. 7 along with the measured values of the different fracture toughness indices discussed earlier. The correlation with the results obtained from specimens that were under plane-strain constraint is excellent. Beyond one cycle, where valid plane-strain tests could not be obtained, the calculated value of the toughness lies between K_{max}^0 and K_{max}^i and the correlation is still reasonable.

d) Fatigue Crack Propagation (FCP). The effect of thermal cycling on FCP was also tentatively evaluated. Tests were run at moderate and high cyclic stress intensity ranges (ΔK) using a load radio of approximately

Table III. Microhardness in the Deformed and Undeformed Region after Aging for Three Hours Following Tensile Deformation

Heat Treatment	Microhardness in Undeformed Region (KHN)	Microhardness in the Necked Region (KHN)
1. Thermally cycled once prior to aging	450^{+2}_{-1}	450^{+5}_{-8}
2. Thermally cycled four times prior to aging	421 ± 12	435^{+20}_{-15}
3. Thermally cycled ten times prior to aging.	362^{+8}_{-12}	601^{+20}_{-15}

15. Crack growth over a known number of cycles was observed. The crack growth intervals were chosen so that the final cyclic stress intensity did not exceed the initial stress intensity by more than 5 pct. The data are shown in Fig. 13 and can be represented by an equation of the form:

$$\frac{da}{dN} = R(\Delta K)^m \qquad [10]$$

where R, m = constants.

A "least squares" line was fit to the data. Values for R and m were calculated and are listed in Table IV. There is essentially no difference between the conventionally treated and singly cycled material. For 4 cycles there was some improvement in the FCP properties. The improvements may be attributed to a combination of decreased tensile strength as predicted by some investigators[34-39] as well as to possible changes in slip character due to the presence of an fcc phase and as reflected in the increased strain hardening exponents for the cycled material.[40-42] The FCP results are in general agreement with those of Miller[42,43] for 300 grade maraging steel.

IV. SUMMARY AND CONCLUSIONS

1) Thermal cycling of a 300 grade maraging steel at a rate of 0.33°C/s, holding at 825°C for two minutes and cooling to room temperature, produced retained austenite in a martensitic matrix. During subsequent aging to strengthen the matrix, the austenite remained stable. Thus, a microstructure consisting of aged martensite and austenite was produced.

2) The fracture toughness of conventionally heat treated material was about 77 MPa$\sqrt{m}$ at a strength level of 1931 MPa. The toughness increased to 116 MPa$\sqrt{m}$ at a strength level of 1655 MPa as a result of a single thermal cycle.

3) In addition to higher fracture toughness as measured by K_{IC}, the fracture mode changed from catastrophically abrupt to gradual as a result of cycling.

4) A model taking into account the mechanical properties of aged martensite and austenite and based on the plastic energy dissipated by a slowly moving crack was invoked. The calculations were in good agreement with the experimental results.

5) Ten thermal cycles resulted in some metastable austenite which transformed to martensite during fracturing. This resulted in an additional increment in toughness but only at a significantly reduced strength level.

6) The fatigue crack propagation properties of the cycled material were only slightly superior to those of the conventionally treated material.

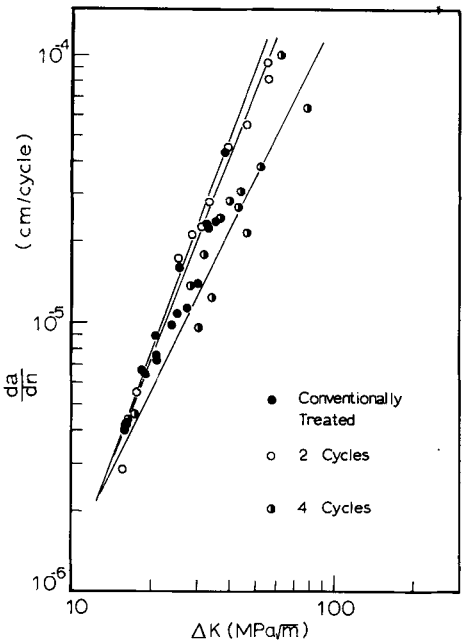

Fig. 13—Crack growth rate as a function of cyclic stress intensity parameter for 3 different heat treatments. The lines represent "least squares" fit to the data.

Table IV. List of Constants for FCP Equation

Heat Treatment	R (cm^7/N^4)	m
1. Solution annealed and aged.	4.0×10^{-21}	2.5
2. Solution annealed cycled twice and aged.	2.2×10^{-21}	2.6
3. Solution annealed cycled four times and aged.	9.4×10^{-21}	2.1

ACKNOWLEDGEMENT

This work was supported in part by a grant from the Air Force Office of Scientific Research.

REFERENCES

1. S. D. Antolovich, P. M. Shete, and G. R. Chanani: *Amer. Soc. Testing Mater., Spec. Tech. Publ. 514,* 1972, pp. 114-34.
2. S. D. Antolovich, K. Kasi, and G. R. Chanani: *Amer. Soc. Testing Mater., Spec. Tech. Publ. 514,* 1972, pp. 135-50.
3. J. Cook and J. E. Gordon: *Proc. Roy. Soc.,* 1964, vol. A282, pp. 508-20.
4. Stephen D. Antolovich and Birindar Singh: *Met. Trans.,* 1971, vol. 2, pp. 2135-41.
5. W. W. Gerberich, P. L. Hemmings, V. F. Zackay, and E. R. Parker: *Fracture 1969,* pp. 288-035, Chapman and Hall Ltd., London, 1969.
6. H. W. Hayden and S. Floreen: *Trans. ASM,* 1968, vol. 61, pp. 474-88.
7. S. Floreen and H. W. Hayden: *Trans. ASM,* 1968, vol. 61, pp. 489-99.
8. S. Floreen, H. W. Hayden, and R. M. Pilliar: *Trans. TMS-AIME,* 1969, vol. 245, pp. 2529-36.
9. W. W. Gerberich and G. S. Baker: *Amer. Soc. Testing Mater., Spec. Tech. Publ. 432,* 1968, pp. 89-99.
10. J. A. Hall, C. M. Pierce, D. L. Ruckle, and R. A. Sprague: *Mater. Sci. Eng.,* 1972, vol. 9, pp. 197-210.
11. R. F. Decker, J. T. Eash, and A. J. Goldman: *Trans. ASM,* 1962, vol. 55, pp. 58-76.
12. W. A. Spitzig, J. M. Chilton, and C. J. Barton: *Trans. ASM,* 1968, vol. 61, pp. 635-39.
13. A. J. Baker and P. R. Swann: *Trans. ASM,* 1968, vol. 57, pp. 1008-11.
14. S. Floreen and G. R. Speich: *Trans. ASM,* 1968, vol. 57, pp. 714-26.
15. S. Floreen: *Met. Rev.,* 1968, vol. 13, pp. 115-28.
16. A. Goldberg: *Trans. ASM,* 1968, vol. 61, pp. 26-xx.
17. A. Goldberg and D. G. O'Connor: *Nature,* 1967, vol. 213, pp. 170-71.
18. A. Goldberg: *J. Iron Steel Inst.,* 1970, vol. 208, pp. 289-97.

19. E-24 Committee Report, *Book of ASTM Standards,* 1970, part 31, pp. 911-27.
20. Ervin E. Underwood: *Metals Eng. Quart.,* 1961, vol. 1, pp. 70-81.
21. S. D. Antolovich, A. Goldberg, and A. Saxena: *J. Iron Steel Inst.,* 1973, vol. 211, pp. 622-27.
22. *Damage Tolerant Design Handbook, MCLC-HB-01,* Materials and Ceramics Information Center, Battelle, Columbus Lab., Air Force Mat. Lab., Air Force Flight Dynamics Lab., 1972.
23. J. E. Srawley and W. F. Brown, Jr.: *Amer. Soc. Testing Mater., Spec. Tech. Publ. 381,* 1965, pp. 133-96.
24. W. A. Spitzig, G. E. Pellissier, C. D. Beachem, A. J. Brothers, M. Hill, and W. R. Warke: *Amer. Soc. Testing Mater., Spec. Tech. Publ. 436,* 1968, pp. 17-31.
25. G. E. Pellisier: *Eng. Fract. Mech.,* 1968, vol. 1, pp. 55-75.
26. H. J. Rack and D. Kalish: *Met. Trans.,* 1971, vol. 2, pp. 3011-20.
27. G. T. Hahn and A. R. Rosenfield: *Amer. Soc. Testing Mater., Spec. Tech. Publ., 432,* 1968, pp. 5-32.
28. G. T. Hahn and A. R. Rosenfield: *Acta Met.,* 1965, vol. 13, pp. 293-306.
29. W. J. McGregor Tegart: *Elements of Mechanical Metallurgy,* p. 21, MacMillan Co., 1966.
30. J. N. Goodier and F. A. Field: *Fracture of Solids,* D. C. Drucker and J. Gilman, eds., pp. 103-18, Interscience Publishers, 1963.
31. D. S. Dugdale: *J. Mech. Phys. Solids,* 1960, vol. 8, pp. 100-06.
32. N. I. Muskhelishvilli: *Some Basic Problems in the Mathematical Theory of Elasticity,* p. 340, Noordhoff, Groningen, Holland, 1953.
33. R. E. Reed Hill: *Physical Metallurgy Principles,* p. 638, D. Van Nostrand Co., 1964.
34. B. Tomkins: *Phil. Mag.,* 1968, vol. 18, pp. 1041-65.
35. G. R. Chanani, S. D. Antolovich, and W. W. Gerberich: *Met. Trans.,* 1972, vol. 3, pp. 2661-72.
36. F. A. McLintok: Discussion on the paper by C. Laird in *Amer. Soc. Testing Mater., Spec. Tech. Publ. 415,* 1967, pp. 170-74.
37. H. W. Liu: *Appl. Mater. Res.,* 1964, vol. 3, pp. 229-37.
38. A. J. McEvily, Jr. and T. L. Johnston: *Int. J. Fract. Mech.,* 1967, vol. 3, pp. 45-73.
39. D. H. Avery and W. A. Backofen: *Fracture of Solids,* D. C. Drucker and J. Gilman, eds., p. 339, Interscience Publishers, 1963.
40. G. A. Miller, D. H. Avery, and W. A. Backofen: *Trans. TMS-AIME,* 1966, vol. 236, pp. 1667-73.
41. C. Laird: *Amer. Soc. Testing Mater., Spec. Tech. Publ. 415,* 1967, pp. 131-68.
42. G. A. Miller: *Trans. ASM,* 1968, vol. 61, pp. 442-48.
43. G. A. Miller: *Trans. ASM,* 1969, vol. 62, pp. 651-58.